SCIENTIFIC REPORTS

OPEN

SUBJECT AREAS:
STRUCTURE OF SOLIDS AND LIQUIDS
METALS AND ALLOYS

Received
31 March 2014

Accepted
23 May 2014

Published
12 June 2014

Correspondence and requests for materials should be addressed to P.Z. (zhang_ping@iapcm.ac.cn)

Nucleation and growth mechanisms of hcp domains in compressed iron

Wei-Wei Pang[1], Ping Zhang[1,2], Guang-Cai Zhang[1], Ai-Guo Xu[1] & Xian-Geng Zhao[1]

[1]Institute of Applied Physics and Computational Mathematics, Beijing 100088, People's Republic of China, [2]Beijing Computational Science Research Center, Beijing 100084, People's Republic of China.

In our previous work, we have pointed out that the shock-induced phase transition in iron occurs with the help of interface energy which reduces the potential barrier between two phases. Here, through studying the nucleation and growth mechanisms of hcp domains in compressed iron, we find that the flatted-octahedral-structure (FOS) is the primary structural unit of the embryo nucleus and phase interface of hcp domains, and the interfacial energy is reduced via formation of FOSs. The phase transition process can be described by the following four stages: (i) Some atoms deviate from their equilibrium positions with the aid of thermal fluctuations to form FOSs with two different deformation directions in the local region; (ii) FOSs with different deformation directions aggregate to form a thin stratified structure like twin-crystal configuration; (iii) The thin stratified structure undergoes a relative slip to form the new hcp phase; (iv) The hcp phase domain grows up through the formation of new FOSs along the phase boundary. In addition, through comparing the time evolution curves of initial single phase domain, we find that the growth rate of single phase domain depends on the loading way and its occurrence time.

Because of its technological, geological, and sociological importance, the states of iron at high pressures have been extensively studied both in theory and experiments[1–4]. One of the most studied parts is the structural phase transition from body-centered-cubic (bcc) into hexagonal-close-packed (hcp) structure that occurs around 13 GPa[5–10]. To date, there are two primary phase transition mechanisms proposed for iron from bcc into hcp structure[11]. The first mechanism is that, the uniaxial compression along [001] crystal direction and expansion along [1$\bar{1}$0] make the (110) crystal plane to transform into hexagon, and then the relative slides between the atomic layers transform the crystal into hcp structure. The second mechanism is that, the shear of (112) crystal plane along the [111] crystal direction forces the atoms of (110) crystal plane to transform into hexagonal arrangement, which results in a compression and small rotation of (110) crystal plane, and then the relative shifts between the (110) crystal planes transform the crystal into hcp structure. Recently, some researches[12,13] have demonstrated that when the shock compression is along the [100] crystal direction, the plane spacing between the (011) planes is not changed due to the lack of the plasticity, and the c/a value is greater than 1.7 in the hcp phase. Whereas, when the shock compression is along the [110] or [111] crystal direction, the hcp and face-centered-cubic (fcc) structures coexist, and the c/a value is close to the ideal value of 1.633.

The atomic arrangement structure under high pressure significantly affects the properties of materials, such as the constitutive relation and equation of state[14]. In the non-equilibrium phase transition process, the mechanical behaviors are coupled with the phase transition process. A complete dynamics model of phase transition in iron crucially requires a deepened knowledge about the nucleation mechanism, growth speed, morphology evolution, etc. In our previous work[15], we have pointed out that it is the interface energy, which reduces the potential barrier between bcc and hcp phases, that motivates the phase transition to successfully proceed. Whereas, the micro-mechanism that how the intermediate defect structures break through the phase transition barrier keeps unsolved up to now. Therefore, it becomes outright important to reveal and clarify the atomic arrangement and the corresponding formation mechanisms of the intermediate defect structures, which compose the embryo nucleus and phase interface of hcp domains.

Inspired by this observation, in this paper, through molecular dynamics simulations, we study the dynamics process of phase transition in compressed iron. We find that the flatted-octahedral-structure (FOS) is the primary structural unit of the embryo nucleus and phase interfaces of hcp domains. The hcp domains nucleate and grow up by means of the formation of FOSs from bcc phase. In addition, we also analyze the growth law of the initial single hcp domain under different loading ways.

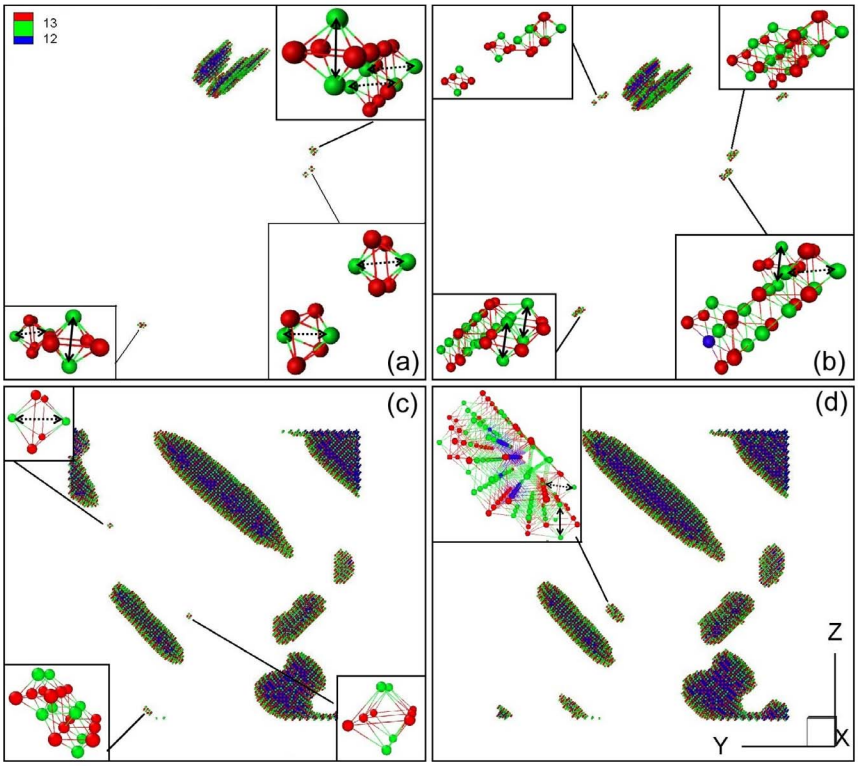

Figure 1 | The dynamics process of phase transition from bcc into hcp structure in iron. Panels (a)–(b) show the formed phase domains under the uniaxial uniform compression, and panels (c)–(d) plot the formed phase domains under the uniaxial shock compression.

Results

The material we use for simulations is single-crystal bcc iron. The simulation tool is the parallel LAMMPS software package[16]. The interatomic interaction is described by an embedded atom method (EAM) potential[17,18], which can well describe the mechanical properties and structural phase transition behaviors of the high-pressure iron. The size of the simulation box is $45.92 \times 22.96 \times 22.96$ nm^3, and contains approximately 2×10^6 atoms. The x, y, and z axes are along the [100], [010], and [001] directions, respectively. In order to analyze and compare the dynamic nucleation and growth processes of hcp domains in iron, we chose two kinds of compression ways along the [100] crystal direction, namely, uniform and shock loading. For uniform compression, the applied strain rate is 10^9/s, and the periodic boundary conditions are applied along three directions to minimize surface and edge effects. For shock compression, the shock wave is generated using the momentum mirror method and the shock velocities is 400 m/s. The periodic boundary conditions are applied along the y and z directions. The atoms are distinguished by calculating their coordination numbers and common neighbor analysis (CNA) values. The single phase domain are extracted using the cluster identification method.

Figure 1 shows the dynamics process of phase transition from bcc into hcp structure in iron. Here, panels (a) and (b) show the formed phase domains under uniaxial uniform compression, while panels (c) and (d) show the formed phase domains under uniaxial shock compression. The blue spheres denote hcp atoms and their coordination numbers are 12; the green and red spheres demote interfacial atoms, and their coordination numbers are 13 and 14, respectively. From the pictures, it is worthy to notice that the nucleation and growth processes of hcp domains under two different loading ways are similar. Firstly, in some local regions where the stress exceeds the phase transition threshold value, some atoms deviate from their equilibrium positions to form defect clusters with the aid of thermal fluctuations. Strikingly, most of these atomic clusters form FOSs, see the insets inside. Interestingly, we observe that there are mainly two kinds of FOSs in the system. The first kind is that two atoms move away along the z direction to become non-neighboring atoms (see the solid arrows). The second kind is that two atoms move away along the y direction to become non-neighboring atoms (as the dashed arrows). Simultaneously, the CNA values of other four atoms which are neighbors with both the two green atoms are changed. According to the CNA values, these atoms are distinguished. We

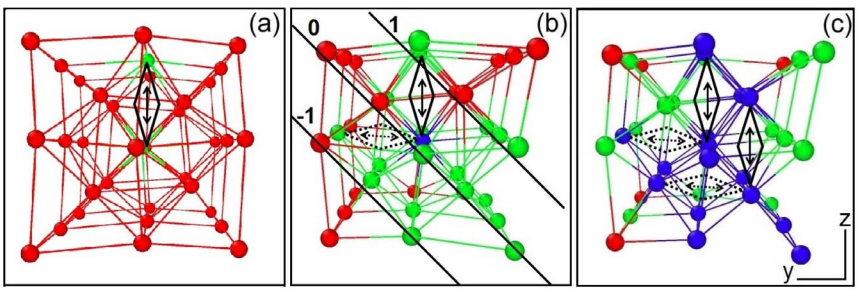

Figure 2 | The nucleation and growth mechanisms of hcp domain by means of the formation of FOSs. Panel (a) shows the structure of formed FOS. Panel (b) shows the nucleation of hcp domain. Panel (c) shows the growth of hcp domain.

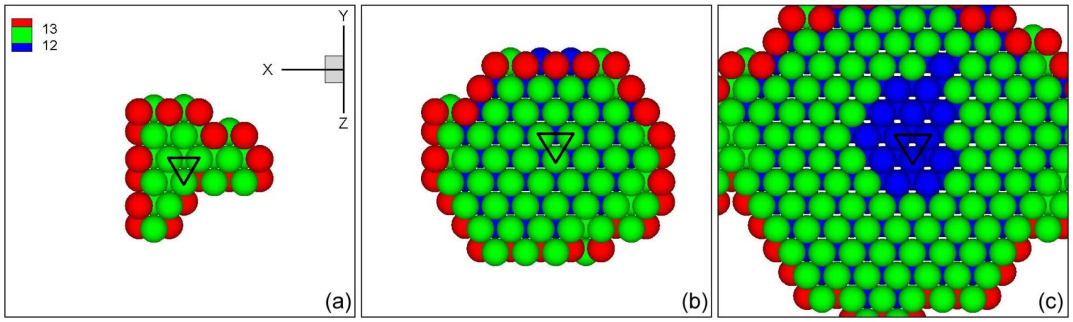

Figure 3 | The relatively slip process between the atomic layers observed from the normal direction of phase plane. Panel (a) shows that some FOSs simply aggregate into a thin stratified structure. Panel (b) shows that the atoms in the central region of the middle layer are transformed into hcp structure. Panel (c) shows that the atoms in the central region of three layers are transformed into hcp structure.

check the cutoff radius used to calculate CNA values, and find that it always can give such FOSs within appropriate cutoff radius range.

To further reveal the formation process of FOSs, we trace these atoms composing FOSs. Remarkably, we find that these atoms occupy the octahedral sites in bcc structure, as shown in Fig. 2(a). Two green atoms of FOS belong to the next nearest neighboring atoms with each other, but belong to the nearest neighboring atoms with the other four red atoms. Thus the interaction between two green atoms is weaker. Under the compression loading along the x direction, to remain the minimum energy state, two body-centered atoms move away along the z axis (or y axis) to form FOS with other four neighboring atoms. These metastable FOSs are dynamical in that they may stochastically occur, annihilate, and reoccur in other places.

With time evolution, some FOSs promote surrounding atoms to further slide and stack into thin stratified structures, see the insets in Fig. 1. Remarkably, due to that the two FOSs with different deforming directions have a co-lattice structure along the [011] or [0$\bar{1}$1] direction, these FOSs tend to stack in the (011) or (0$\bar{1}$1) crystal plane by a co-lattice way to reduce the energy. When the size of this thin stratified structure exceeds a certain value, the central-region atoms of the cluster undergo a relative inter-layer slip, which further reduces the mismatch energy, to become new hcp phase structure. Figure 2(b) shows the formation process of the hcp phase, where the numbers ($\bar{1}$, 0, 1) denote adjacent three layers of atoms. When one atom of the middle layer (0—layer) and one atom of upper layer (1—layer) move away along the z axis to form the first kind of FOS, simultaneously and one atom of below layer ($\bar{1}$—layer) move away along the y axis to form the second kind of FOS, this atom transforms from bcc into hcp structure, as the blue atom shown in Fig. 2(b). This kind of arrangement structure is similar to the twin crystal configuration. Figure 2(c) shows that the three layers of atoms have been gradually transformed into hcp structure by this way. The atoms of the same layer form the first kind of FOSs with the atoms of upper layer, and form the second kind of FOSs with the atoms of lower layer. Such arrangements make that the atoms of the whole layer are gradually transformed into hcp structure. The atoms of adjacent

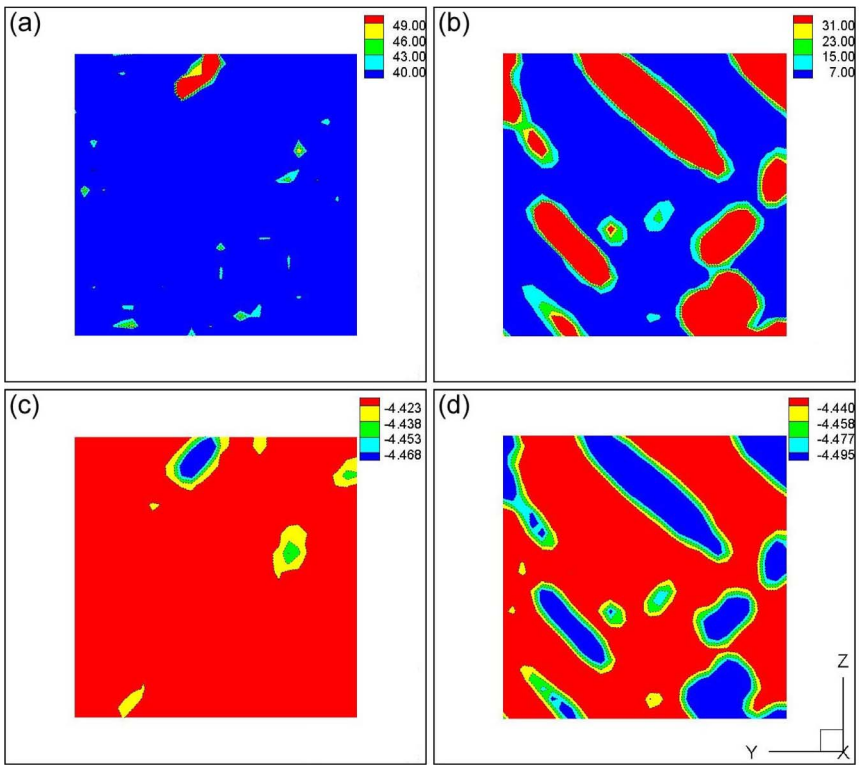

Figure 4 | The temperature and potential energy distributions for two different loading ways. Panels (a)–(b) are the temperature distributions, while panels (c)–(d) are corresponding potential energy distributions.

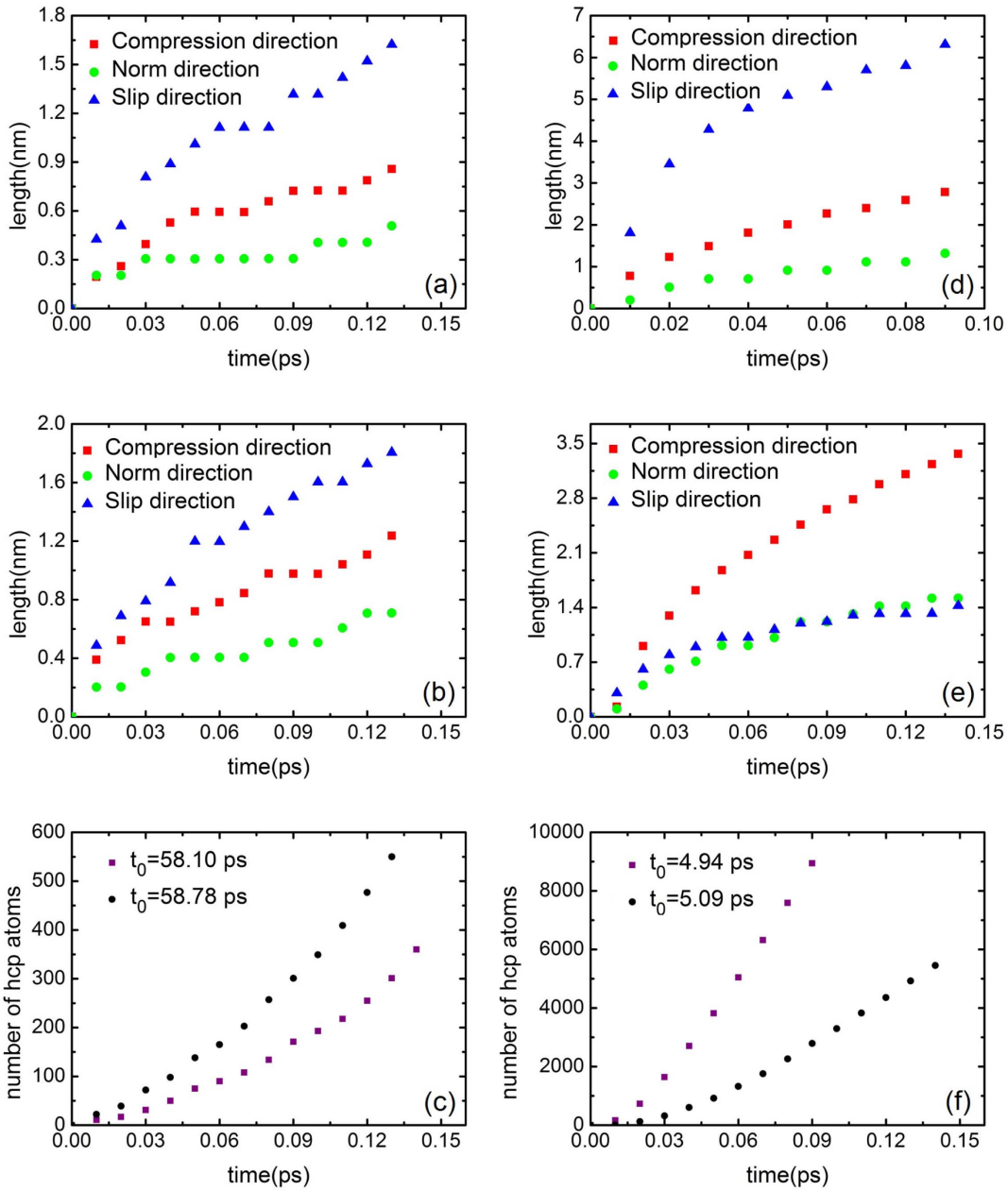

Figure 5 | The lengths of single phase domain along the compression, norm and slip directions, and the total atomic numbers with the growth time. Here, the compression direction is [100], the normal (slip) directions are [011] ([01$\bar{1}$]), [01$\bar{1}$] ([011]), [011] ([01$\bar{1}$]), and [01$\bar{1}$] ([011]) for panels (a), (b), (d), and (e), respectively, and t_0 denotes the moment that the hcp phase domain occurs. Panels (a)–(c) are uniaxial uniform compression, panels (d)–(f) are uniaxial shock compression.

upper layer further form the second kind of FOSs with the atoms of its upper layer to transform themselves into hcp structures. The relatively alternate arrangements between the atomic layers make the phase domain to gradually grow up. These processes of FOS generation, aggregation and slip can be regarded as two steps, wherein the generation and aggregation of FOSs correspond to the formation of perfect hexagon, while the slip of FOSs corresponds to the relative slides between the atomic layers. From an overall consideration, therefore, our proposed mechanism is consistent with the first mechanism proposed in the introduction part. Experimentally, these processes of FOS generation, aggregation and slip are possibly observed from the fine structure of diffraction peaks during bcc-hcp phase transition in the future high-time-resolution X-ray diffraction measurements.

Such a nucleation and growth process of hcp domain also can be observed from several successive snapshots, Figs. 3, which are plotted in the way that one sees from the normal direction of phase plane. Before inter-layer slip happens, as shown in Fig. 3(a), one can see that these atoms of simply aggregated FOSs scarcely overlap, leaving two little holes (see the white region surrounded by black triangle). Whereas, in Fig. 3(b), each two little holes in the central region merge into a small slit (see the white region surrounded by black triangle). Such phenomenon indicates that there is a relative slide between the atomic layers. The CNA values show that the atoms of the middle layer have been transformed into hcp structure. With the further alternate slide between atomic layers, the three layers of defect atoms are gradually transformed into hcp structure, as the central region shown in Fig. 3(c). These atoms leave a larger gap.

From above dynamic nucleation and growth processes of hcp domains, we present that the FOS is the primary structural unit of the embryo nucleus and phase interface of hcp domains. To further understand the formation of FOS, we picked out a layer from Figs. 1(b) and 1(d), respectively, with a thickness of 1.3 nm, perpendicular to the loading direction. Figures 4(a) and 4(c) represent the temperature and potential energy distributions of the layer under uniaxial uniform compression, and Figs. 4(b) and 4(d) represent the temperature and potential energy distributions of the layer under uniaxial shock compression. Here, the temperature is calculated following the expression $\sum_i^n \frac{1}{2} m(\mathbf{v}_i - \bar{\mathbf{v}})^2 = \frac{3}{2} nkT$, where the summation is over a spherical region with the radius being triple crystal lattice constants, $\mathbf{v}_i$ is the atomic velocity, $\bar{\mathbf{v}}$ is the average velocity, and k is the Boltzmann constant. From Fig. 4, it is obvious that the temperature distributions, which surround the single FOS, the thin stratified cluster of FOSs, and the interface of new phase domains, are higher than those in the bcc region. This indicates that the FOS is activated with the help of collective thermal fluctuations. Whereas, the potential energy distributions, which surround the single FOS, the thin stratified cluster of FOSs, and the interface of new phase domains, lie in amplitude between those in the regions of two energy extreme states (bcc and hcp). Thus, it is now clear that the FOS is a metastable structure and acts as a medium of two phase transformation to reduce the potential barrier. As a result, the old (bcc) phase is gradually transformed into the new (hcp) phase through the generation, aggregation and slip of FOS clusters.

The nucleation and growth mechanisms of hcp domain under two different loading ways are the same. we turn now to discuss that the growth rate of initial hcp domain formed under two different compression ways. The length along the [100], [011], [0$\bar{1}$1] directions and the total atomic numbers with the growth time are calculated and analyzed for multiple hcp domains. Figure 5 shows the calculated results for four domains which form at different times or under different loading ways. Here, panels (a)–(c) are the evolution curves under uniaxial uniform compression, while panels (d)–(f) are the evolution curves under uniaxial shock compression. One can observe from Fig. 5 that the evolution law of single hcp domain prominently depends on the loading way and its occurrence time. Under uniaxial uniform compression, the growth rate for domains occurring later is faster. Such a phenomenon might result from that the nucleation sites of hcp domains are randomly located in the system, and when the simulation box is continually compressed, the pressure surrounding the phase domains gradually increases. However, under the uniaxial shock compression, the hcp domains first occur in the earliest region swept by shock wave, namely, the nucleation sites of hcp domains are limited in certain region. Furthermore, the growths of existed phase domains would result in that the pressure of nucleation region decreases. Therefore, the growth rate for domains occurring later is slower. Based on the lengths of single hcp domain along the three directions, we approximately calculated the average linear growth rate of hcp domain. It is found that under uniaxial uniform compression, the average growth rate of single hcp domain is supersonic along the compression and slip directions, whereas, it is subsonic along the normal direction of phase plane. This phenomenon indicates that the morphology of single phase domain in the uniaxial uniform compressed iron is lamellar. Whereas, under uniaxial shock compression, the average growth rate of single hcp domain is supersonic along the three directions, and the stress wave has no time to propagate in the hcp domain. This phenomenon indicates that the morphology of single phase domain in the uniaxial shock compressed iron is ellipsoid-like.

Discussion

The phase transition processes of iron from bcc into hcp structure under uniaxial compression along [100] direction has been investigated via molecular dynamic simulations. Based on the common neighbor analysis and cluster identification method, the dynamic nucleation and growth processes of hcp domains are analysed in detail. We present that the FOS is the primary structural unit of the embryo nucleus and phase interface of hcp domains. The hcp domains nucleate and grow up by means of the generation, aggregation and slip of FOSs from old phase. The nucleation and growth processes can be described by four stages: Firstly, some atoms deviate from their equilibrium positions to form two kinds of FOSs with different deformation directions. Secondly, some FOSs with two different deformation directions aggregate to form a thin stratified structure which arranges in a twin-crystal configuration way. Thirdly, when the size of the thin stratified defect cluster exceeds certain value, it undergoes a relative slide to generate new phase structure. Fourthly, the hcp domains gradually grow up with the aid of the formation of new FOSs along the phase boundary. In addition, we also discussed the growth rate of initial hcp domain formed in compressed iron. It is found that the growth rate of a single hcp domain significantly depends on the loading way and its occurrence time.

Methods

Two methods have been employed in our numerical simulations and data analysis: (i) The numerical MD simulations are performed using the well-known LAMMPS software package. The interatomic interactions used in the simulations are described by embedded atom method potentials. (ii) The atoms are distinguished by the common neighbor analysis (CNA) method. The single phase domain atoms are extracted using the cluster identification method.

1. Bancroft, D., Peterson, E. L. & Minshall, S. Polymorphism of iron at high pressure. *J. Appl. Phys.* **27**, 291–298 (1956).
2. Boettger, J. C. & Wallace, D. C. Metastability and dynamics of the shock-induced phase transition in iron. *Phys. Rev. B* **55**, 2840–2849 (1997).
3. Germann, T. C. *et al.* Orientation dependence in molecular dynamics simulations of shocked single crystals. *Phys. Rev. Lett.* **84**, 5351–5354 (2000).
4. Liu, J. B. & Johnson, D. D. Bcc-to-hcp transformation pathways for iron versus hydrostatic pressure: coupled shuffle and shear modes. *Phys. Rev. B* **79**, 134113 (2009).
5. Kadau, K., Germann, T. C., Lomdahl, P. S. & Holian, B. L. Microscopic view of structural phase transitions induced by shock waves. *Science* **296**, 1681–1684 (2002).
6. Kadau, K. *et al.* Shockwaves in polycrystalline iron. *Phys. Rev. Lett.* **98**, 135701 (2007).
7. Mathon, O. *et al.* Dynamics of the magnetic and structural $\alpha - \varepsilon$ phase transition in iron. *Phys. Rev. Lett.* **93**, 255503 (2004).
8. Sandoval, L., Urbassek, H. M. & Entel, P. Solid-solid phase transitions and phonon softening in an embedded-atom method model for iron. *Phys. Rev. B* **80**, 214108 (2009).
9. Wang, B. T. *et al.* Molecular dynamics simulations of hcp/fcc nucleation and growth in bcc iron driven by uniaxial compression. *J. Phys.: Condens. Matter* **21**, 435404 (2009).
10. Cui, X. L. *et al.* Phase transformation of iron under shock compression: effects of voids and shear stress. *Phys. Rev. B* **78**, 024115 (2008).
11. Wang, F. M. & Ingalls, R. Iron bcc-hcp transition: local structure from x-ray-absorption fine structure. *Phys. Rev. B* **57**, 5647–5654 (1998).
12. Kalantar, D. H. *et al.* Direct observation of the $\alpha - \varepsilon$ transition in shock-compressed iron via nanosecond X-ray diffraction. *Phys. Rev. Lett.* **95**, 075502 (2005).
13. Hawreliak, J. A. *et al.* High-pressure nanocrystalline structure of a shock-compressed single crystal of iron. *Phys. Rev. B* **78**, 220101 (2008).
14. Preston, D. L., Tonks, D. L. & Wallace, D. C. Model of plastic deformation for extreme loading conditions. *J. Appl. Phys.* **93**, 211–220 (2003).
15. Pang, W. W. *et al.* Morphology and growth speed of hcp domains during shock-induced phase transition in iron. *Sci. Rep.* **4**, 3628 (2014).
16. Plimpton, S. Fast parallel algorithms for short-range molecular dynamics. *J. Comp. Phys.* **117**, 1–19 (1995).
17. Daw, M. S. & Baskes, M. I. Embedded-atom method: derivation and application to impurities, surfaces, and other defects in metals. *Phys. Rev. B.* **29**, 6443–6453 (1984).
18. Harrison, R., Voter, A. F. & Chen, S. P. [Embedded Atom Potential For bcc Iron] Atomistic Simulation Of Materials: Beyond Pair Potentials. [Vitek, V. & Srolovitz, D. J. (ed.)] [219–222] (Plenum Press, New York, 1989).

Acknowledgments

We acknowledge support of the National Magnetic Confinement Fusion Science Program of China under Grant 2012GB106001 and Science Foundation of CAEP under Grants No. 2011A0301016 and No. 2012B0101014.

Author contributions

W.W.P. did the calculations. P.Z., G.C.Z., A.G.X. and X.G.Z. analyzed the results. W.W.P., G.C.Z. and P.Z. wrote the paper. P.Z. and G.C.Z. were responsible for project planning and execution.

Additional information

Competing financial interests: The authors declare no competing financial interests.

How to cite this article: Pang, W.-W., Zhang, P., Zhang, G.-C., Xu, A.-G. & Zhao, X.-G. Nucleation and growth mechanisms of hcp domains in compressed iron. *Sci. Rep.* **4**, 5273; DOI:10.1038/srep05273 (2014).